Cyclotriphosphorus Complexes: Solid-State Structures and Dynamic Behavior of Monoadducts with Carbonyl Fragments

Massimo Di Vaira, Markus P. Ehses, and Piero Stoppioni*

Dipartimento di Chimica, Università di Firenze, via Maragliano 77, 50144 Firenze, Italy

Maurizio Peruzzini

I.S.S.E.C.C., C.N.R., via J. Nardi 39, 50132 Firenze, Italy

Received November 29, 1999

Treatment of the *cyclo*-P_3 complexes [(triphos)MP_3] [triphos = 1,1,1-tris(diphenylphosphinomethyl)ethane; M = Co (**1**), Rh (**2**)] with stoichiometric amounts of $[M'(CO)_5(thf)]^{n+}$ ($n = 0$, M′ = Cr, Mo, W; $n = 1$, M′ = Re) and $[W(CO)_4(PPh_3)(thf)]$ yields the compounds [{(triphos)M}($\mu,\eta^{3:1}$-P_3){$M'(CO)_5$}] [M = Co; M′ = Cr (**3a**), Mo (**3b**), W (**3c**). M = Rh; M′ = W (**4**)], [{(triphos)Co}($\mu,\eta^{3:1}$-P_3){$Re(CO)_5$}]BF_4·C_7H_8 (**5**) and [{(triphos)Rh}-($\mu,\eta^{3:1}$-P_3){$W(CO)_4PPh_3$}]·$2CH_2Cl_2$ (**6**). The X-ray structures of **5** and **6** have been determined. Crystal data: **5**, monoclinic space group $P2_1/n$, $a = 14.754(2)$ Å, $b = 24.886(4)$ Å, $c = 15.182(2)$ Å, $\beta = 103.38(1)°$, $Z = 4$; **6**, monoclinic space group $P2_1/n$, $a = 14.872(3)$ Å, $b = 27.317(6)$ Å, $c = 16.992(4)$ Å, $\beta = 111.75(5)°$, $Z = 4$. The effects of η^1 coordination on the MP_3 core are discussed by comparing the MP_3 skeletons in the above structures with those of the previously characterized bis and tris end-on adducts of organometallic fragments of **1**. Variable temperature NMR data for the compounds provide evidence for fluxional processes in solution that may be interpreted as {(triphos)M} rotation about its C_3 axis and {$M'(CO)_5$} or {$M'(CO)_4PPh_3$} scrambling over the P_3 cycle. The activation parameters of the fragment scrambling process are determined.

Introduction

Transition metal complexes with ligands consisting of unsubstituted main group atoms have attracted large interest over the past decades.[1] The characterization of the compounds in the solid state by X-ray diffraction analysis has revealed a large variety of polyatomic open chain or cyclic units that are generally unstable as uncoordinated species. The complexes with P_n ligands are especially the focus of current research. The favorable NMR features of the ^{31}P nucleus allow the investigation of structural properties of the compounds in solution. These studies often reveal unexpected dynamic behavior consisting of (i) skeleton rearrangements of multinuclear cluster compounds,[2] (ii) relative rotation of parts of the molecule about symmetry or pseudosymmetry axes,[3] and (iii) scrambling of coordinated fragments.[2g,3a,4]

In our laboratories, a series of neutral[5] and cationic[6] compounds (Chart 1) have been described in which a cyclic triatomic E_3 or E_2X (E = P, As; X = S, Se) ligand is η^3-bound to a metal atom of the cobalt or of the nickel group, which in turn bears the tripodal tridentate 1,1,1-tris(diphenylphosphinomethyl)ethane (triphos) as coligand. In these complexes the phosphorus atoms in both the triphos and the cyclic main-group ligand are chemically and magnetically equivalent, which is traced to the rotation of the two ligands (triphos and cyclic

Chart 1

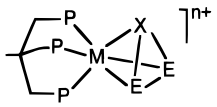

n = 0; M = Co, Rh, Ir; E = X = P

n = 1; M = Ni, Pd, Pt; E = X = P

n = 1; M = Co; E = P, As; X = S, Se

(1) (a) Herrmann, W. A. *Angew. Chem., Int. Ed. Engl.* **1986**, *25*, 56. (b) Roesky, H. W., Ed. *Rings, Clusters and Polymers of Main Group and Transition Elements*; Elsevier: Amsterdam, 1989. (c) Wachter, J. *Angew. Chem., Int. Ed. Engl.* **1998**, *37*, 750. (d) Scherer, O. J. *Acc. Chem. Res.* **1999**, *32*, 751. (e) Whitmire, K. H. *Adv. Organomet. Chem.* **1998**, *42*, 2.

(2) (a) Scherer, O. J.; Berg, G.; Wolmershäuser, G. *Chem. Ber.* **1995**, *128*, 635. (b) Barth, A.; Huttner, G.; Fritz, M.; Zsolnai, L. *Angew. Chem., Int. Ed. Engl.* **1990**, *29*, 929. (c) Scherer, O. J.; Braun, J.; Walther, P.; Wolmershäuser, G. *Chem. Ber.* **1992**, *125*, 2661. (d) Scherer, O. J.; Mohr, T.; Wolmershäuser, G. *J. Organomet. Chem.* **1997**, *529*, 379. (e) Scherer, O. J.; Schwarz, G.; Wolmershäuser, G. *Z. Anorg. Allg. Chem.* **1996**, *622*, 951. (f) Friedrich, G.; Scherer, O. J.; Wolmershäuser, G. *Z. Anorg. Allg. Chem.* **1996**, *622*, 1478. (g) Scherer, O. J.; Berg, G.; Wolmershäuser, G. *Chem. Ber.* **1996**, *129*, 53.

(3) (a) Di Vaira, M.; Ehses, M. P.; Peruzzini, M.; Stoppioni, P. *J. Organomet. Chem.* **2000**, *593*−*594*, 127. (b) Scherer, O. J.; Werner, B.; Heckmann, G.; Wolmershäuser, G. *Angew. Chem., Int. Ed. Engl.* **1991**, *30*, 553. (c) Scherer, O. J.; Schwalb, J.; Wolmershäuser, G. *New J. Chem.* **1989**, *13*, 399. (d) Scherer, O. J.; Winter, R.; Wolmershäuser, G. *Z. Anorg. Allg. Chem.* **1993**, *619*, 827. (e) Scheer, M.; Becker, U. *J. Organomet. Chem.* **1997**, *545*−*546*, 451. (f) Barbaro, P.; Peruzzini, M.; Ramirez, J. A.; Vizza, F. *Organometallics* **1999**, *18*, 4237.

(4) Scheer, M.; Leiner, E.; Kramkowski, P.; Schiffer, M.; Baum, G. *Chem.*−*Eur. J.* **1998**, *4*, 1917.

(5) (a) Ghilardi, C. A.; Midollini, S.; Orlandini, A.; Sacconi, L. *Inorg. Chem.* **1980**, *19*, 301. (b) Bianchini, C.; Mealli, C.; Meli, A.; Sacconi, L. *Inorg. Chim. Acta* **1979**, *37*, L543. (c) Mealli, C.; Midollini, S.; Moneti, S.; Sacconi, L. *Cryst. Struct. Commun.* **1980**, *9*, 1017.

(6) (a) Di Vaira, M.; Sacconi, L.; Stoppioni, P. *J. Organomet. Chem.* **1983**, *250*, 183. (b) Di Vaira, M.; Peruzzini, M.; Stoppioni, P. *J. Chem. Soc., Dalton Trans.* **1984**, 359. (c) Di Vaira, M.; Innocenti, P.; Moneti, S.; Peruzzini, M.; Stoppioni, P. *Inorg. Chim. Acta* **1984**, *83*, 161. (d) Di Vaira, M.; Peruzzini, M.; Stoppioni, P. *Polyhedron* **1986**, *5*, 945.

10.1021/ic991380w CCC: $19.00
Published on Web 04/15/2000

triatomic unit) with respect to each other. The main-group atoms are generally reactive toward organic or organometallic fragments possessing Lewis acidic properties. The added moieties, depending on their ligating properties, bind in η^1, η^2, or η^3 fashion to the cyclic triatomic ring. While the equivalence of the triphos and P_3 phosphorus atoms in the diamagnetic triple decker compounds $[\{(triphos)M\}(P_3)\{M(triphos)\}]^+$ (M = Ni, Rh, Pd)[7] is interpretable in terms of relative rotation of the decks, the equivalence of the *cyclo*-P_3 P atoms in compounds bearing η^1 or η^2 binding metal fragments must involve exchange between different coordination sites.[3,8] This process does not seem to be influenced by the extent of the interaction between the added metal moiety and the MP_3 core,[8] since the slow-exchange limit of the NMR spectrum has almost never been reached on cooling the solutions. In contrast to the transition metal adducts, η^1 or η^2 complexes formed by the interaction of $[(triphos)MP_3]$ and $[(triphos)Co(As_2S)]BF_4$ with unsaturated organic reagents do not exhibit processes of the above type iii even at elevated temperatures.[9] A low-temperature limit for transition metal adducts of $[(triphos)MP_3]$ has been reached for the first time with the pentacarbonyl bis adducts $[\{(triphos)Co\}(\mu,\eta^{3:1:1}\text{-}P_3)\{M'(CO)_5\}_2]$ [M′ = Cr (**7a**), Mo (**7b**), W (**7c**)].[3a] Distinct dynamic processes could be frozen, which were interpreted in terms of {(triphos)Co} rotation about its C_3 axis, metal carbonyl fragment migration on the P_3 cycle, and a concerted motion of the pentacarbonyl substituents. Severe line broadening and the simultaneous occurrence of the various dynamic processes prevented a complete analysis of the behavior in solution.

In this paper we report the synthesis and variable temperature NMR studies of the monoadducts $[\{(triphos)M\}(\mu,\eta^{3:1}\text{-}P_3)\{M'(CO)_5\}]$ [M = Co; M′ = Cr (**3a**), Mo (**3b**), W (**3c**). M = Rh; M′ = W (**4**)], $[\{(triphos)Co\}(\mu,\eta^{3:1}\text{-}P_3)\{Re(CO)_5\}]BF_4\cdot C_7H_8$ (**5**), and $[\{(triphos)Rh\}(\mu,\eta^{3:1}\text{-}P_3)\{W(CO)_4PPh_3\}]\cdot 2CH_2Cl_2$ (**6**), as well as the structure determinations of **5** and **6**. The exocyclic coordination of only one carbonyl fragment to the cyclic P_3 unit was expected to reduce the number of possible kinetic modes, and the replacement of the quadrupolar cobalt by rhodium was expected to reduce the broadening of the ^{31}P resonances. To study possible effects of increased steric hindrance on the dynamic processes, a CO ligand was replaced by a triphenylphosphine in the tungsten pentacarbonyl. The solid-state structures of **5** and **6** extend the series of structural studies of the compounds $[(triphos)M(P_3)\{M'(CO)_4L\}_n]$ (L = CO, PR_3; $n = 1-3$),[3a,5a,5c] among which terms with $n = 1$ were previously missing. The additional data have provided more information on the effects that end-on coordination exerts on the geometry of the MP_3 pseudotetrahedral core.

Results and Discussion

Syntheses, Reactivity, and IR Properties of the Compounds. The dinuclear complexes **3a**, **3b**, **3c**, **4**, **5**, and **6** can be regarded as the monoadducts of the carbonyl fragments $\{M'(CO)_5\}^{n+}$ ($n = 0$; M′ = Cr, Mo, W. $n = 1$; M′ = Re) and $\{W(CO)_4(PPh_3)\}$ of the *cyclo*-P_3 ligand in **1** and **2**. They are synthesized by adding the stoichiometric amount of the appropriate solvent-stabilized 16VE fragment to the P_3 complex in THF. The formation of the adducts occurs immediately, as revealed by IR monitoring of the reaction. After workup the complexes are isolated in moderate to high yields as orange to yellow solids. The cobalt derivatives are moderately soluble in toluene, the rhodium complexes are very soluble in aromatic solvents, whereas all compounds are very soluble in CH_2Cl_2 and THF. They are stable under an inert atmosphere and may be handled in air for a limited time.

The group 6 pentacarbonyl fragments may be displaced in a few hours by treatment with an excess of triphenylphosphine in boiling THF, re-forming **1** and **2** in addition to the substitution products $[M(CO)_5(PPh_3)]$ (NMR and IR monitoring). Thermal as well as photochemical treatment of the pentacarbonyl tungsten complex **4** yields an orange solid that is insoluble in common organic solvents; this is probably a $\{W(CO)_4\}$ adduct, as suggested by the IR spectrum of the reaction mixture. A solution of **4** in CH_2Cl_2 or $CHCl_3$ remains substantially unchanged for weeks, whereas the phosphine-substituted **6** in $CHCl_3$ solution decomposes in the same period, forming an insoluble, not yet characterized, blue precipitate. As described for the bis adducts,[3a] no detachment reaction is observed for the group 6 pentacarbonyl compounds under an atmosphere of carbon monoxide; such behavior has been observed also for $[M(CO)_5(PR_3)]$ complexes.[10]

The CO streching bands in the IR solution spectra (see the Experimental Section) exhibit shapes and relative intensities similar to those of appropriate phosphine complexes,[11] with the expected shift to higher wavenumbers for the cationic Re compound. This suggests donor/acceptor properties of the naked phosphorus atoms in the "ligand" $\{(triphos)MP_3\}$ that are similar to those of phosphines. The absorptions of each complex are slightly shifted to lower frequencies with respect to those of the corresponding bis adduct.

X-ray Structure Analyses of $[\{(triphos)Co\}(\mu,\eta^{3:1}\text{-}P_3)\{Re(CO)_5\}]BF_4\cdot C_7H_8$ (5) and $[\{(triphos)Rh\}(\mu,\eta^{3:1}\text{-}P_3)\{W(CO)_4(PPh_3)\}]\cdot 2CH_2Cl_2$ (6). The X-ray structure determinations of **5** and **6** have provided the first structural data for end-on monoadducts of metal−carbonyl fragments on phosphorus atoms of the MP_3 core. The structures of bis and tris adducts have already been reported.[3a,5a,c] A view of the cation in **5** is shown in Figure 1, and a view of the molecule in **6** appears in Figure 2. Selected values of bond distances and angles are given in Tables 1 (**5**) and 2 (**6**). The MP_3 moieties exhibit consistent distortions from the idealized trigonal symmetry upon substitution, with the M−P bond involving the substituted P atom definitely shorter [by 0.051 Å (**5**) and 0.059 Å (**6**)] and the other two M−P bonds overall slightly longer [by 0.01 Å (**5**), 0.02 Å (**6**)] than the (symmetry-related) bonds in the respective (**1** or **2**, in the above order) parent compound. There are consistent differences also among the P−P bonds of each structure, although these differences are less pronounced than the previous ones probably because the P−P bonds are shorter and stronger than the M−P ones. In particular, the two P−P bonds formed by the substituted P atom are shorter than the third bond of the P_3 cycle. The same trend (although magnified) in distances was found for the $[(triphos)Co(P_3Me)]^+$ cation.[9a] Related trends have been observed for the cores of the compounds bearing two metal carbonyl substituents,[3a,5a] where the M−P bonds formed by the substituted P atoms and the P−P bond between the same atoms

(7) (a) Di Vaira, M.; Midollini, S.; Sacconi, L. *J. Am. Chem. Soc*. **1979**, *101*, 1757. (b) Bianchini, C.; Di Vaira, M.; Meli, A.; Sacconi, L. *J. Am. Chem. Soc*. **1981**, *103*, 1448. (c) Dapporto, P.; Sacconi, L.; Stoppioni, P. *Inorg. Chem*. **1981**, *20*, 3834.

(8) (a) Di Vaira, M.; Rovai, D.; Stoppioni, P. *Polyhedron* **1990**, *20*, 2477. (b) Di Vaira, M.; Peruzzini, M.; Stoppioni, P. *J. Chem. Soc., Dalton Trans*. **1990**, 109. (c) Di Vaira, M.; Stoppioni, P. *Polyhedron* **1994**, *13*, 3045.

(9) (a) Capozzi, G.; Chiti, L.; Di Vaira, M.; Peruzzini, M.; Stoppioni, P. *J. Chem. Soc., Chem. Commun*. **1986**, 1799. (b) Di Vaira, M.; Niccolai, L.; Peruzzini, M.; Stoppioni, P. *Organometallics* **1985**, *4*, 1988.

(10) Darensbourg, D. J.; Graves, A. H. *Inorg. Chem*. **1979**, *18*, 1257.

(11) Verkade, J. G. *Coord. Chem. Rev*. **1973**, *9*, 1.

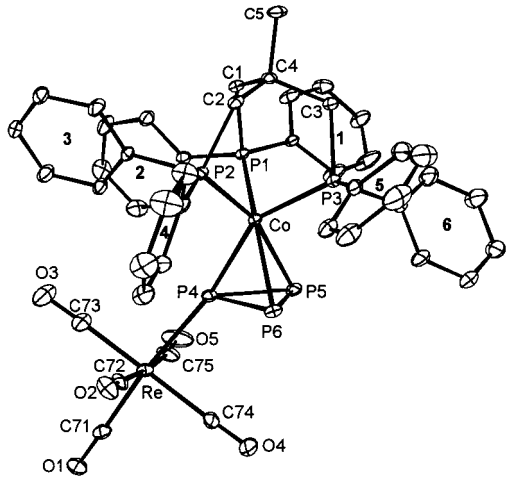

Figure 1. ORTEP drawing of the cation in the structure of [{(triphos)Co}($\mu,\eta^{3:1}$-P_3){$Re(CO)_5$}]BF_4·C_7H_8 (**5**) with 10% probability ellipsoids. Phenyl rings are identified by numbers for clarity.

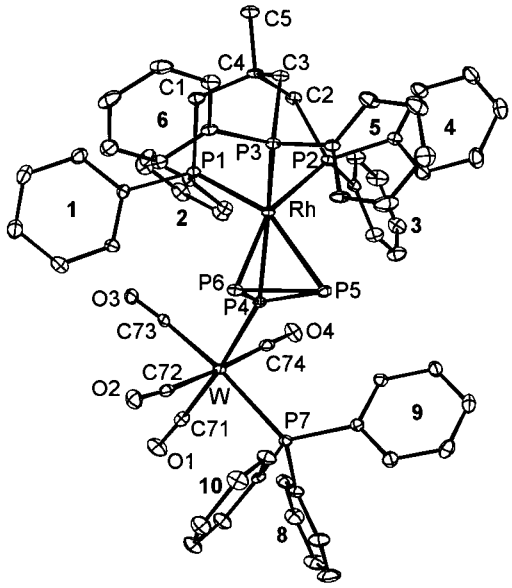

Figure 2. ORTEP drawing of the dinuclear molecule in the structure of [{(triphos)Rh}($\mu,\eta^{3:1}$-P_3){$W(CO)_4PPh_3$}]·$2CH_2Cl_2$ (**6**) with 10% probability ellipsoids. Phenyl rings are identified by numbers for clarity.

were found to be shorter than the other bonds of the corresponding type.

As before,[3a,9a] the results of extended Hückel (EH) calculations[12] on undistorted models of the present compounds are consistent with the above trends, yielding slightly higher values of the overlap population for the bonds of the pseudotetrahedral MP_3 unit, which are found to shorten upon addition of the metal carbonyl group(s). However, at variance with the case of the simple methyl substitution,[9a] when metal carbonyls are involved as substituents, it seems impossible to relate the results of the calculations to a single orbital interaction of outstanding importance. For the present compounds it appears that both a release of antibonding contributions (particularly for the P−P bonds which shorten) and an increase of bonding contributions (to the shortening of an M−P bond) among high-energy occupied MO's may be effective. On the other hand, calculations on a model for the possible triple substitution in **1** with metal carbonyls yielded slightly lower M−P overlap population values than for the unsubstituted parent compound, suggesting that the 0.028 Å overall lengthening of the M−P(P_3) bonds detected on going from **1** to the trisubstituted derivative[5c] should be attributed to electronic factors rather than to the effects of steric repulsions.

(12) (a) Hoffmann, R. *Angew. Chem., Int. Ed. Engl*. **1982**, *21*, 711. (b) Mealli, C.; Proserpio, D. M. *J. Chem. Educ.* **1990**, *67*, 399.

Table 1. Selected Bond Lengths (Å) and Angles (deg) for [{(triphos)Co}($\mu,\eta^{3:1}$-P_3){$Re(CO)_5$}]BF_4·C_7H_8 (**5**)

Co−P(1)	2.208(2)	Co−P(6)	2.312(2)
Co−P(2)	2.203(2)	P(4)−P(5)	2.126(3)
Co−P(3)	2.195(2)	P(4)−P(6)	2.129(3)
Co−P(4)	2.250(2)	P(5)−P(6)	2.143(3)
Co−P(5)	2.333(2)	Re−P(4)	2.513(2)
P(1)−Co−P(2)	91.62(8)	P(3)−Co−P(4)	148.54(9)
P(1)−Co−P(3)	94.55(8)	P(5)−P(4)−P(6)	60.46(11)
P(2)−Co−P(3)	91.69(8)	P(4)−P(5)−P(6)	59.84(10)
P(1)−Co−P(6)	156.58(9)	P(4)−P(6)−P(5)	59.70(10)
P(2)−Co−P(5)	161.18(9)	Co−P(4)−Re	170.15(9)

Table 2. Selected Bond Lengths (Å) and Angles (deg) for [{(triphos)Rh}($\mu,\eta^{3:1}$-P_3){$W(CO)_4PPh_3$}]·$2CH_2Cl_2$ (**6**)

Rh−P(1)	2.285(2)	P(4)−P(5)	2.132(3)
Rh−P(2)	2.317(2)	P(4)−P(6)	2.142(3)
Rh−P(3)	2.290(2)	P(5)−P(6)	2.162(3)
Rh−P(4)	2.359(2)	W−P(4)	2.542(2)
Rh−P(5)	2.445(2)	W−P(7)	2.523(2)
Rh−P(6)	2.412(3)		
P(1)−Rh−P(2)	91.02(9)	P(5)−P(4)−P(6)	60.75(11)
P(1)−Rh−P(3)	91.55(8)	P(4)−P(5)−P(6)	59.86(10)
P(2)−Rh−P(3)	87.70(7)	P(4)−P(6)−P(5)	59.39(10)
P(1)−Rh−P(5)	153.96(8)	Rh−P(4)−W	151.32(10)
P(2)−Rh−P(6)	157.99(9)	P(4)−W−P(7)	92.34(7)
P(3)−Rh−P(4)	153.34(8)		

The $Re(CO)_5$ group in **5** is arranged rather symmetrically with respect to the [(triphos)CoP_3] moiety, with the best line through O(2), C(72), Re, C(75), and O(5) almost parallel to the P(5)−P(6) direction [the two lines form a 5.1(1)° angle] and with two P(n)−P(4)−Re (n = 5, 6) angles of comparable magnitude (Table 1). Such an arrangement is predicted by the EH calculations to be the most favorable, although the rotational barrier about the Re−P bond is very low. In the structures of compounds where two metal carbonyl groups are attached to atoms of the P_3 moiety the arrangements are less symmetrical because of repulsions between the groups.[3a,5a] The least symmetrical arrangement exists in **6** (Table 2), where it is probably caused by intramolecular interactions and by the effects of packing forces on the bulky PPh_3 substituent on the tungsten atom. The same factors may be responsible for the small value, 151.3(1)°, of the Rh−P(4)−W angle in **6**, compared to the 161.1° mean of the Co−P−M′ angles (M′ = W,[3a] Cr,[5a] Mn[5c]) in the compounds with two or three metal carbonyl substituents on P_3. On the other hand, the large Co−P(4)−Re angle, 170.1(1)°, in **5** is not easily rationalized, unless it is attributed to the effect of short intramolecular contacts [e.g., O(3)···C(35), 3.30(1) Å, involving a carbon atom of phenyl group no. 3 in Figure 1]. The W−P(4) distance, 2.542(2) Å, in **6** matches the mean, 2.554(7) Å, of the two analogous distances in the disubstituted compound[3a] and is only slightly longer than the 2.523(2) Å W−P(7) distance formed by tungsten with the PPh_3 phosphorus in **6**.

NMR Properties of the Compounds. The $^{31}P\{^1H\}$ NMR spectra of compounds **3**−**6** at room temperature show two signals (Tables 3 and 4) that occur in the regions for the phosphorus atoms of triphos and P_3. In the spectrum of **6** a further signal, due to the triphenylphosphine, appears at low field with respect to the triphos resonance. The signal of the

Table 3. ^{31}P NMR Data of the Compounds [{(triphos)Co}($\mu,\eta^{3:1}$-P_3){M(CO)$_5$}] [M = Cr (**3a**), Mo (**3b**), W (**3c**)] and [{(triphos)Co}($\mu,\eta^{3:1}$-P_3){Re(CO)$_5$}]BF_4·C_7H_8 (**5**) at Different Temperatures[a]

compd	T (K)	δ ($P_{triphos}$)	δ ($P_{cyclo-P_3}$)	$^1J_{PP}$
3a	333	34.0 (br, 3P)	−250.0 (br, 3P)	
	190	34.1 (br, 3P)	−179.8 (tr,1P),[b]	309
			−292.0 (d, 2P)	
3b	273	34.2 (br, 3P)	267.5 (br, 3P)	
	190	34.4 (br, 3P)	−219.4 (tr, 1P),	304
			−292.7 (d, 2P)	
3c	298	33.9 (br, 3P)	−275.1 (br, 3P)	
	190	33.7 (s, br, 3P)	−239.8 (tr, 1P),[c]	301
			−294.9 (d, 2P)	
5	298	33.1 (br, 3P)	−294.7 (br, 3P)	
	176	33.1 (br, 3P)	−266.3 (ddm, 1P),	304
			−307.6 (dm, br, 2P)	

[a] CD_2Cl_2; δ (ppm); J (Hz); br = broad; dm = doublet of multiplets; ddm = doublet of doublets of multiplets; tr = triplet. [b] Even-numbered fine splitting: 7 Hz. [c] $^1J_{WP}$ = 190 Hz.

triphos P atoms in all of the cobalt derivatives sharpens on lowering the temperature without change in the chemical shift, which is also unaffected by the nature of the complexing metal carbonyl. The P_3 resonance of the neutral cobalt complexes exhibits the expected high-field shifts with increasing atomic number of the group 6 metal; the shifts are less pronounced than those of the corresponding bis adducts.[3a]

When the temperature is lowered to 190 K, the P_3 resonances of compounds **3a**−**c**, after running through coalescence [T_c (K): **3a**, 280; **3b**, 225; **3c**, 240], split into a triplet and a doublet with an integral ratio of 1:2. The observed multiplicities and the intensity ratios allow us to attribute the low-field triplet to the end-on coordinated P, which is deshielded by the electron-withdrawing 16VE fragment. Furthermore, the presence of satellites in the **3c** triplet, due to $^1J_{PW}$ coupling, confirms the direct connection of this P atom to the tungsten. The value of 190 Hz for this coupling constant lies in the range spanned by other {W(CO)$_5$} end-on adducts of naked phosphorus atoms [$^1J_{PW}$ (Hz): [{Cp*Ni}$_2$(μ_4-P_2){W(CO)$_5$}$_2$], 86;[13] [{Cp*W(CO)$_2$}$_2$(μ_4-P_2){W(CO)$_5$}$_2$], 197;[14] [{^{t}Bu$_3$C$_5$H$_2$)Co}$_2$(P_4){W(CO)$_5$}$_2$], 242[2g]], all these values being smaller than the $^1J_{PW}$ values for [W(CO)$_5$(PR_3)].[15] The P−P coupling constants (Tables 3 and 4) are slightly larger than those found for the bis adducts[3a] but are in the range reported for other P_3 complexes.[3c,9a,16] As the atomic number of the metal in the carbonyl fragment increases, the triplet shifts upfield, thus approaching the resonance of the unsubstituted P atoms, which remains practically unchanged at ca. −293 ppm. Also, the P_3 resonance of the cationic rhenium derivative, **5**, coalesces on lowering the temperature to 190 K [T_c (K): 260], before splitting into two resonances with an integral ratio of 1:2 (Table 3, Figure 3). By analogy with the spectra of the neutral pentacarbonyl adducts, the low-field signal, centered at −266.3 ppm, is attributed to the coordinated P atom and that at −307.6 ppm to the two unsubstituted phosphorus atoms. The small line widths of these signals, which appear as a pseudotriplet and a pseudodoublet, allow detection of a fine structure that may be interpreted according to an A_3DEE' spin system (A = triphos P, D = substituted, E and E′ = unsubstituted P_3 atoms) in which the naked P atoms are not magnetically equivalent. The attainment of this limit may be favored by the short intramolecular contacts revealed by the structure investigation of the solid compound.

The room temperature ^{31}P NMR spectra of the rhodium complexes **4** and **6** (Table 4) are affected by partial coalescence. The fast-exchange limit at higher temperature was reached at a weaker field in order to minimize decomposition. Under these conditions small line widths allow observation of multiplet fine structures, and the presence of quartets for both the triphos and the P_3 signals confirms the chemical and magnetic equivalence of the P atoms within each set. These atoms are additionally coupled to rhodium, with coupling constants comparable to those found for the parent compound **2**.[6a] The P_3 resonances in **6** are doubled because of the presence of the PPh_3 substituent. The phosphine resonance in **6** appears as a complex multiplet because of the coupling with the substituted P atom of the P_3 unit and with the three equivalent P atoms of the triphos coligand. The latter long-range coupling is proved by a fine structure with a similar coupling constant in the triphos signals; its value (4 Hz) is smaller than that found for [{(triphos)Ni}($\mu,\eta^{3:2}$-P_3){Pt(PPh_3)$_2$}]$^+$ ($^4J_{PP}$ = 47 Hz)[8c] probably because of the significantly different electronic environment of the phosphine-bearing metal atom in the two compounds.

When the temperature is lowered [T_c (K): **4**, 250; **6**, 280], significant changes occur for all of the signals in the spectra of the rhodium compounds. The low-field resonance in **6**, due to the triphenylphosphine, appears as a doublet of doublets with coupling constants of 28 and 12 Hz. The larger of these is assigned to the coupling ($^2J_{PP}$) with the end-on bound P atom of the P_3 unit; such coupling is in fact in the range found for *cis*-[W(CO)$_4$(PR_3)(PR'_3)] complexes.[17] The other one is likely due to coupling with one of the triphos P atoms. The triphos resonances in both **4** and **6** are doubled by coupling with rhodium, and each component consists of two groups of partly overlapping signals. Each of these signals exhibits a complex fine pattern containing a larger number of lines in the **6** than in the **4** system (because of the PPh_3 ligand in the former compound). The P_3 resonances in these low-temperature spectra consist of two multiplets having a 1:2 intensity ratio: a low-field triplet and a higher-field doublet whose components are split into several lines. The P_3 $^1J_{PP}$ coupling constants for **4** and **6** are similar, and the $^1J_{PW}$ of **4** has the same value as that found for **3c**. The above patterns of signals have not been solved because of their complexity, but they clearly suggest that the dynamic processes are frozen at the low temperature. The pseudodoublet of **6** at −282.3 ppm (due to the unsubstituted *cyclo*-P_3 phosphorus atoms) approaches coalescence at about 180 K, but the slow exchange limit was not reached even at the lowest accessible temperature (176 K). However, the separation of ca. 1000 Hz between the two humps that appear at that temperature is too large to be due to P−P coupling. Rather, it is indicative of two separate signals, possibly due to different environments of the free P atoms of the *cyclo*-P_3, similar to the arrangement found in the X-ray structure.

The ^{1}H NMR spectra of the compounds (see the Experimental Section) are very similar to each other and are substantially unchanged on lowering the temperature to 190 K. This suggests that the equivalence of sites of the triphos ligand on the ^{1}H

(13) Scheer, M.; Schuster, K.; Krug, A.; Hartung, H. *Chem. Ber*. **1996**, *129*, 973.
(14) Scherer, O. J. In *Multiple Bonds and Low Coordination in Phosphorus Chemistry*; Regitz, M., Scherer, O. J., Eds.; Thieme: Heidelberg, Germany, 1990; p 112.
(15) Pregosin, P. S.; Kunz R. W. In *NMR, Basic Principles and Progress*; Diehl, P., Fluck, E., Kosfeld, R., Eds.; Springer-Verlag: Berlin, Germany, 1979; Vol. 16, p 99.
(16) Scherer, O. J.; Braun, I.; Wolmershäuser, G. *Chem. Ber*. **1990**, *123*, 471.
(17) Reference 16, p 115. Boyles, M. L,; Brown, D. V.; Drake, D. A.; Hostetler, C. K.; Maves, C. K.; Mosbo, J. A. *Inorg. Chem*. **1985**, *24*, 3126.

Table 4. ^{31}P NMR Data of the Compounds [{(triphos)Rh}($\mu,\eta^{3:1}$-P_3){W $(CO)_5$}] (**4**) and [{(triphos)Rh}($\mu,\eta^{3:1}$-P_3){$W(CO)_4(PPh_3)$}]·$2CH_2Cl_2$ (**6**) at Different Temperatures[a]

compd	T (K)	δ ($P_{triphos}$)	δ ($P_{cyclo-P_3}$)	δ (P_{Ph_3})
4	343[b]	11.5 (dq, 3P, $^1J_{PRh}$ = 135, $^2J_{PP}$ = 19.5	−273.2 (dq, 3P, $^1J_{PRh}$ = 32.2, $^1J_{PW}$ = 64.2)	
	183	18.4 (dm, 3P, $^1J_{PRh}$ = 131.7)	−240.7 (tm, 1P, $^1J_{PP}$ = 308, $^1J_{PW}$ = 193)	
			−291 (dm, 2P)	
6	350[b]	11.3 (dqd, 3P, $^1J_{PRh}$ = 136.5, $^2J_{PP}$ = 19.1, $^4J_{PP}$ = 4.0)	−267.4 (dqd, 3P, $^1J_{PRh}$ = 28.0, $^2J_{PPh3}$ = 30)	16.3 (m, 1P)
	198	18.1 (dm, 3P, $^1J_{PRh}$ = 135)	−239.4 (tm, 1P, $^1J_{PP}$ = 316)	22.6 (dd, 1P, $^2J_{PP}$ = 27.8,
			−282.3 (dm, 2P)	$^4J_{PP}$ = 12.5, $^1J_{PW}$ = 233.2
	176	19.3 (m, 3P)	−239.5 (tm, 1P, $^1J_{PP}$ = 310)	22.6 (m, 1P)
			−277.0 (m, 1P)	
			−290.0 (m, 1P)	

[a] δ (ppm); J (Hz); 81.02 MHz, if not otherwise stated, CD_2Cl_2; m = multiplet, dm = doublet of multiplets, dd = doublet of doublets, dq = doublet of quartets, dqd = doublet of quartets of doublets, tm = triplet of multiplets. [b] 32.20 MHz, $CDCl_3$.

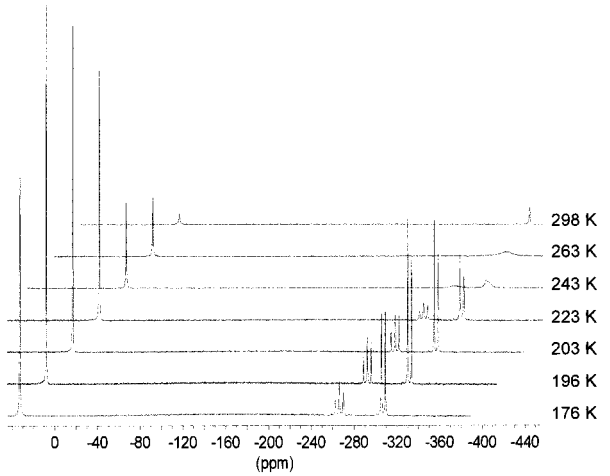

Figure 3. ^{31}P{^{1}H} NMR spectra of [{(triphos)Co}($\mu,\eta^{3:1}$-P_3){Re-$(CO)_5$}]BF_4·C_7H_8 (**5**) at different temperatures (CD_2Cl_2, 81.02 MHz).

NMR time scale is preserved even at low temperature and is at variance with the behavior observed for the bis adducts **7a**−**c**, where the methylene proton signals at low temperature split into two broad bands with a 1:2 intensity ratio.[3a]

In the carbonyl region of the room temperature ^{13}C{^{1}H} NMR spectra of the **3**−**5** pentacarbonyl complexes (see the Experimental Section) the absorptions split into two resonances, which are attributed to the cis- and trans-configured carbonyls with respect to the P_3 group. Because of the presence of the triphenylphosphine in **6**, three carbonyl resonances are observed, in agreement with the coordination geometry around tungsten. The larger C−P coupling constants of the carbonyls trans to the P atoms compare favorably with literature reports on phosphine complexes.[15] The resonance due to the other four CO groups in the pentacarbonyl compounds is sufficiently intense to show satellites due to direct C−W coupling with the expected values.[15] A remarkable feature is the quartet structure of the CO ligand trans to the *cyclo*-P_3, which is due to coupling to three equivalent P nuclei. Combined with the temperature independence of the ^{1}H NMR spectra of the present compounds, noted above, this points to a lower barrier to the metal carbonyls motion in the monoadducts than in the bis-adducts, due to reduced steric hindrances.

As far as the component of motion consisting of *cyclo*-P_3 rotation around the pseudo-3-fold axis of the (triphos)MP_3 part of the compound is concerned, a higher rotational barrier may be expected for the rhodium complexes than for the cobalt ones in view of the rigid conformation found for **4** and **6** at low temperature and of the higher temperatures needed to reach their fast-exchange limit. This is also in keeping with the results of the NMR studies on cyclopropenyl complexes [(triphos)M(C_3-Ph_3)]PF_6,[18] (M = Ni, Pd, Pt), which have revealed dynamic features similar to those of *cyclo*-P_3 derivatives.[3c] The rotational barrier for the cyclopropenyl complexes increases with the atomic number of the transition metal, while the steric effects appear to be of limited importance. On the other hand, the presence of bulky metal carbonyl fragments in the P_3 derivatives seems to affect the above motion because the slow-exchange limit, never reached for the unsubstituted parents,[6a] has been reached for the derivatives with two[3a] and three substituents.[3c] The presence of only one fragment does not seem to raise the barrier sufficiently in the case of the cobalt complexes to block the triphos vs P_3 rotation.

Table 5. Activation Parameters for the Metal Scrambling Process of the {$M(CO)_5$} Fragment along the P_3 Ligand in Complexes [{(triphos)Co}($\mu,\eta^{3:1}$-P_3){$M(CO)_5$}] [M = Cr (**3a**), Mo (**3b**), W (**3c**)] from Variable Temperature ^{31}P{^{1}H} NMR Spectra

	3a	**3b**	**3c**
$\Delta H^{\ddagger}$ (kJ mol^{-1})	63.2	61.6	65.9
$\Delta S^{\ddagger}$ (J mol^{-1} K^{-1})	66.8	96.0	103.4
$\Delta G^{\ddagger}_{298}$ (kJ mol^{-1})	43.5	33.1	35.0
k_{298} (s^{-1})	1.62×10^5	1.00×10^7	1.45×10^6

[a] From Eyring plot of [ln(k/T) vs $1/T$].

Activation Parameters and Considerations of the {M(CO)$_4$L}-Scrambling Mechanism. A line shape analysis of the multiplets due to the P_3 phosphorus atoms has been performed using the program CAHOS[19] for the series of neutral cobalt complexes. The activation parameters have been derived from an Eyring plot and are reported in Table 5. The data obtained through consideration of the changes of the signals with temperature are attributed to the migration of the end-on coordinated metal pentacarbonyl fragment between the P_3 sites, although steric interactions between the {$M(CO)_5$} moieties and the phenyl groups of the triphos coligand may affect the kinetics. The activation enthalpy $\Delta H^{\ddagger}$ is found to be essentially the same (ca. 63 kJ mol^{-1}) for the three compounds **3a**−**c**. In pentacarbonyl complexes of the type [$M(CO)_5$L] (M = Cr, Mo, W) the M−L bond strength is more sensitive to the steric bulk of L rather than to the nature of the metal.[20] The present results show that the molybdenum and the tungsten derivatives behave very similarly, exhibiting close activation entropies and exchange

(18) (a) Hughes, R. P.; Tucker, D. S.; Rheingold, A. L. *Organometallics* **1993**, *12*, 3069. (b) Ghilardi, C. A.; Innocenti, P.; Midollini, S.; Orlandini, A.; Vacca, A. *J. Chem. Soc., Dalton Trans.* **1995**, 1109. (c) Churchill, M. R.; Fettinger, J. C.; McCullough, L. G.; Schrock, R. R. *J. Am. Chem. Soc.* **1984**, *106*, 3356.
(19) Cecconi, F.; Ghilardi, C. A.; Innocenti, P.; Midollini, S.; Orlandini, A.; Ienco, A.; Vacca, A. *J. Chem. Soc., Dalton Trans.* **1996**, 2821.
(20) Zhang, S.; Dobson, G. R. *Inorg. Chim. Acta* **1991**, *181*, 103.

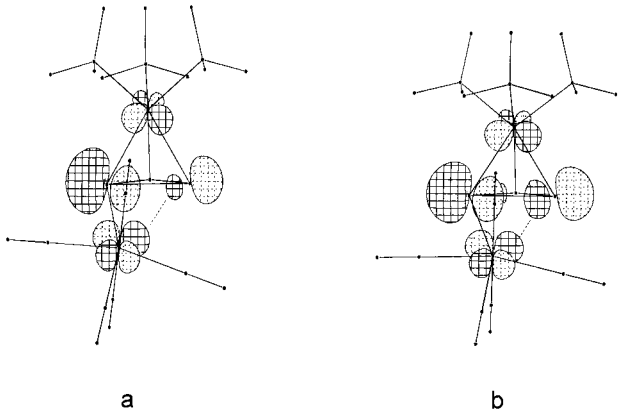

Figure 4. Important atomic orbital contributions, from EH calculations, to the HOMO for two steps of a possible path for $W(CO)_5$ migration along a P−P edge. A bonding W···P interaction (dashed line) sets up at a distance and increases as the two atoms approach.

rates at room temperature. The activation entropy increases from the chromium to the molybdenum derivative and is positive for all compounds, suggesting a transition state with a higher degree of disorder compared to the starting situation. The $\Delta G^{\ddagger}$ values, which range from 33.1 to 43.5 kJ mol^{-1}, are smaller than the $\Delta G^{\ddagger} \approx 50$ kJ mol^{-1} determined for the transfer process of the $\{W(CO)_5\}$ groups between the two phosphorus end-on coordination sites in the dimetalladiphosphatetrahedrane $[\{Cp^*(OC)_2W\}_2(P_2)\{W(CO)_5\}]$.[4] A $\Delta G^{\ddagger}$ value (32.6 kJ mol^{-1}) similar to that found for **3b** and **3c** was determined for the scrambling process in the insertion product $[\{(triphos)Ni\}(\mu,\eta^{3:2}\text{-}P_3)\{Pt(PPh_3)_2\}]^+$.[8c] The negative activation entropy, −53.9 J mol^{-1} K^{-1}, for the platinum compound, which contrasts with the positive values obtained for the pentacarbonyl derivatives, is suggestive of different kinetic pathways for the unidentate adducts and the insertion product and may also be due to grossly interchanged roles for the equilibrium and the transition states in the two cases.

Simple EH calculations on a $[(triphos)MP_3]$ model with one attached $W(CO)_5$ group suggest that the metallotropic shifts in the present compounds should proceed along the P−P edges rather than over the P_3 triangular face. The essential orbital contributions to the HOMO for two steps along a possible path of the former type are depicted in Figure 4. A bonding W···P interaction is seen to be switched on at some distance of the tungsten atom from the target phosphorus while antibonding contributions (Figure 4a) to the original W−P interaction build up. The process is easied by a slight opening of the P−P bond, which contributes to produce a shallow energy minimum at the intermediate point of such path. However, a barrier exists along the path from the experimental solid-state arrangement to a configuration similar to that of Figure 4a. Presumably, the barrier is lowered by suitable deformations of the metal carbonyl moiety along the path.

1,2-Metallotropic shifts undergone by unsaturated complex fragments between atoms with free lone pairs have been reported, although scarcely for compounds containing pairs of P atoms as part of tetrahedral cores[3a,4] or of more complex structures.[2a,21] However, no shifts of this type have been detected at room temperature for systems containing the pentaphosphorus ring, although static structures of the η^1-type[22] and η^2-type[23] have been characterized in the solid state. Apparently, small differences in electron density distributions may have significant effects on the extent of the barriers to the motion of the metal carbonyl groups.

Experimental Section

All reactions and manipulations were performed under an atmosphere of dry oxygen-free argon. THF was freshly distilled from potassium. Dichloromethane, hexane, SiO_2 (act. II−III), and Al_2O_3 (neutral, act. I) for chromatography were degassed and flushed with argon prior to use. The infrared spectra were recorded on a Perkin-Elmer Spectrum BX spectrometer using a KBr cell. The $^{31}P\{^1H\}$ (^1H; $^{13}C\{^1H\}$) NMR spectra were measured in CD_2Cl_2 solution on a Bruker AC 200 spectrometer at 81.02 MHz (200.13; 50.32 MHz) and on a Varian FT-80 spectrometer at 32.20 MHz. Phosphorus-31 (hydrogen-1; carbon-13) positive chemical shifts are to high frequency relative to that of 85% H_3PO_4 as an external standard (relative to TMS as an internal standard) at 0.0 ppm. The NMR spectral simulation was performed by means of the computer program CAHOS, which allows the simultaneous refinement of chemical shifts, line widths, and homo- and heteronuclear coupling constants.[19] Analytical data for carbon and hydrogen were obtained from the Microanalytical Laboratory of the Department of Chemistry of the University of Firenze. The hexacarbonyl complexes were used as purchased, and $[(triphos)CoP_3]$ (**1**)[5a] and $[(triphos)RhP_3]$ (**2**)[5b] were synthesized according to the literature methods. Compound **3a** was synthesized with a slightly modified procedure compared to that reported in the literature.[5a]

Syntheses of $[\{(triphos)Co\}(\mu,\eta^{3:1}\text{-}P_3)\{M(CO)_5\}]$ [M = Cr (3a), Mo (3b), W (3c)]. To a yellow solution of 200 mg (0.26 mmol) of $[(triphos)CoP_3]$ (**1**) in 200 mL of THF is added at room temperature (rt) under stirring an equimolar amount of the appropriate solvent adduct $[M(CO)_5(thf)]$ in THF freshly prepared via rt photolysis of the hexacarbonyl in a Pyrex Schlenk tube {$[Cr(CO)_6]$, 15 min; $[Mo(CO)_6]$, 80 min; $[W(CO)_6]$, 20 min} in ca. 45 mL of THF. The color of the solution immediately changes to orange-red. After about 1 h the reaction is completed (IR monitoring). The solvent is removed under a stream of inert gas and the residue redissolved in ca. 3 mL of CH_2Cl_2 and transferred onto a column (water-cooled, 1 × 20 cm, SiO_2, in *n*-hexane). The products were eluted with hexane/CH_2Cl_2 = 2/1 as orange to red bands, giving fibrous red solids on evaporating the solvents. They may be purified by slow precipitation from hexane/CH_2Cl_2 by reducing the volume of the solution in a light stream of inert gas. Yields: 38% (**3a**); 66% (**3b**); 77% (**3c**). Anal. Calcd for **3a**, $C_{46}H_{39}CoCrO_5P_6$: C, 57.0; H, 4.06. Found: C, 56.1; H, 4.40. Anal. Calcd for **3b**, $C_{46}H_{39}CoMoO_5P_6$: C, 54.6; H, 3.88. Found: C, 56.3; H, 4.47. Anal. Calcd for **3c**, $C_{46}H_{39}CoO_5P_6W$: C, 50.2; H, 3.57. Found: C, 50.1; H, 4.00. NMR [δ (ppm), J (Hz)]. **3a**, ^1H, 298 K: 7.8−6.8 (m, Ph, 30H), 2.33 (s, br, CH_2, 6H), 1.30 (s, br, CH_3, 3H). 190 K: 7.7−6.7 (m, br, Ph, 30H), 2.21 (br, CH_2, 6H,), 1.40 (br, CH_3, 3H). $^{13}C\{^1H\}$, 298 K: 218.5 (s, *cis*-CO), 138.9 (m, *i*-Ph), 132.4 (m, *o*-Ph), 129.6 (m, *p*-Ph), 128.8 (m, *m*-Ph), 34.8 (m, CH_2), 38.1 (m, CH_3), 37.1 (m, C). **3b**, ^1H, 298 K: 7.8−6.7 (m, Ph, 30H), 2.30 (s, br, CH_2, 6H), 1.50 (s, br, CH_3, 3H). $^{13}C\{^1H\}$, 298 K: 211.5 (q, *trans*-CO, $^4J_{CP}$ = 10.4), 206.8 (s, *cis*-CO), 140.9 (m, *i*-Ph), 133.0 (m, *o*-Ph), 129.1 (m, *p*-Ph), 128.4 (m, *m*-Ph), 35.2 (m, CH_2), 38.5 (q, CH_3, $^3J_{PC}$ = 9.7), 37.4 (q, C, $^2J_{CP}$ = 5.4). **3c**, ^1H, 298 K: 7.8−6.8 (m, Ph, 30H), 2.37 (s, br, CH_2, 6H), 1.31 (s, br, CH_3, 3H). 190 K: 8.0−6.5 (m, br, Ph, 30H), 2.21 (br, CH_2, 6H), 1.40 (br, CH_3, 3H). $^{13}C\{^1H\}$, 298 K: 199.8 (q, *trans*-CO, $^4J_{CP}$ = 10.4), 198.2 (s, *cis*-CO, $^1J_{CW}$ = 128.5), 139.0 (m, *i*-Ph), 132.4 (m, *o*-Ph), 129.7 (m, *p*-Ph), 128.8 (m, *m*-Ph), 35.0 (m, CH_2), 38.4 (q, CH_3, $^3J_{CP}$ = 9.6), 37.2 (q, C, $^2J_{CP}$ = 4.8). IR [CH_2Cl_2; ν (cm^{-1})]. **3a**: 2057(m), 1982(w), 1937(vs), 1912(sh). **3b**: 2068(m), 1988(w), 1944(vs), 1905(sh). **3c**: 2066(m), 1979(w), 1935(vs), 1901(sh).

Synthesis of $[\{(triphos)Co\}(\mu,\eta^{3:1}\text{-}P_3)\{Re(CO)_5\}]BF_4\cdot C_7H_8$ (5). $[Re(CO)_5]BF_4$ is prepared following the procedure described for the trifluoromethanesulfonato derivative[24] using 0.17 g (0.87 mmol) of $AgBF_4$ and 0.36 g (0.90 mmol) of $[Re(CO)_5Br]$ in 25 mL of CH_2Cl_2.

(21) Müller, C.; Bartsch, R.; Fischer, A.; Jones, P. G. *Polyhedron* **1993**, *12*, 1383.
(22) Scherer, O. J.; Brück, T.; Wolmershäuser, G. *Chem. Ber.* **1989**, *122*, 2049.
(23) Detzel, M.; Friedrich, G.; Scherer, O. J.; Wolmershäuser, G. *Angew. Chem., Int. Ed. Engl.* **1995**, *34*, 1321.

The filtered solution of $[Re(CO)_5]BF_4$ is added dropwise to a solution of 0.69 g (0.89 mmol) of [(triphos)CoP_3] in 50 mL of CH_2Cl_2. An immediate color change from yellow to red indicates spontaneous formation of the monoadduct. The reaction is completed after 1 h (IR monitoring). **5** is isolated by adding toluene (ca. 20 mL) and reducing the volume of the solution in a light stream of inert gas, giving an orange-red microcrystalline solid. Yield: 36%. Anal. Calcd for **5** ($C_{53}H_{47}BCoF_4O_5P_6Re$): C, 49.7; H, 3.70. Found: C, 49.1; H, 3.65. NMR [δ (ppm), J (Hz)]. ^{1}H, 298 K: 7.31−7.05 (m, Ph, 30H), 2.45 (s, br, CH_2, 6H), 1.62 (q, $^4J_{HP}$ = 2.6, CH_3, 3H). 176 K: 7.5−6.8 (m, br, Ph, 30H), 2.35 (br, CH_2, 6H), 1.49 (br, CH_3, 3H). ^{13}C{^{1}H}, 298 K: 179.0 (s, CO), 137.5 (m, *i*-Ph), 132.1 (br, *o*-Ph), 130.5 (s, *p*-Ph), 129.2 (s, *m*-Ph), 34.4 (m, CH_2), 38.1 (q, CH_3, $^3J_{PC}$ = 10.2), 37.4 (q, C, $^2J_{CP}$ = 4.2). IR [CH_2Cl_2; ν (CO) (cm^{-1})]: 2148(m), 2088(w), 2048(vs), 2027(m). IR [Nujol; ν (cm^{-1})]: 2152(vs), 2102(vs), 2056(vs), 2038-(vs), 2008(s), 1971(w) (CO), 1053 (vs) (BF).

Synthesis of [{(triphos)Rh}(μ,$\eta^{3:1}$-P_3){$W(CO)_5$}]·$2CH_2Cl_2$ (4). Compound **4** is prepared as described above for the cobalt analogue **3c** using 90 mg (0.11 mmol) of [(triphos)RhP_3] (**2**) in 200 mL of THF. After about 2 h the reaction is completed (IR monitoring). Workup as above leaves a yellow microcrystalline solid. It may be recrystallized from hexane/CH_2Cl_2 by reducing the volume of the solution under a light stream of inert gas. Yield: 70%. Anal. Calcd for $C_{46}H_{39}O_5P_6RhW$: C, 48.3; H, 3.44. Found: C, 49.11; H, 3.55. NMR [δ (ppm), J (Hz)]. ^{1}H, 298 K: 7.4−7.0 (m, Ph, 30H), 2.31 (m, CH_2, 6H), 1.50 (q, $^4J_{HP}$ = 2.8, CH_3, 3H). 190 K: 7.4−6.8 (m, Ph, 30 H), 2.21 (br, CH_2, 6H), 1.38 (br, CH_3, 3H). ^{13}C{^{1}H}, 298 K: 199.9 (q, *trans*-CO, $^4J_{CP}$ = 10.5), 192.2 (s, *cis*-CO, $^1J_{CW}$ = 126.7), 138.0 (dd, *i*-Ph, $^1J_{CP}$ = 27, $^2J_{CRh}$ = 15), 132.6 (br, *o*-Ph), 129.9 (s, *p*-Ph), 128.9 (br, *m*-Ph), 34.7 (m, CH_2), 39.3 (q, CH_3, $^3J_{PC}$ = 9.9), 38.7 (q, C, $^2J_{CP}$ = 3.8). IR [CH_2-Cl_2; ν (cm^{-1})]: 2066(m), 1980(w), 1935(vs), 1903(sh).

Synthesis of [{(triphos)Rh}(μ,$\eta^{3:1}$-P_3){$W(CO)_4(PPh_3)$}] (6). To a yellow solution of 100 mg (0.12 mmol) of [(triphos)RhP_3] (**2**) in 25 mL of THF is added at rt under stirring an equimolar amount of [$W(CO)_4(PPh_3)$(thf)] in THF (freshly prepared via rt photolysis of 90 mg (0.14 mmol) of [$W(CO)_5(PPh_3)$] in ca. 30 mL of THF in a Pyrex Schlenk tube for 15 min.[25] After about 4 h the reaction is completed (IR monitoring). The workup is performed as described above, giving a yellow crystalline solid. It may be recrystallized from hexane/CH_2-Cl_2 by reducing the volume of the solution under a light stream of inert gas. Yield: 52%. Anal. Calcd for **6** ($C_{65}H_{58}O_4P_7RhWCl_4$): C, 50.4; H, 3.78. Found: C, 50.7; H, 3.80. NMR [δ (ppm), J (Hz)]. ^{1}H, 298 K: 7.70−7.55 (m, *o*-Ph(PPh_3), 6H), 7.4−7.0 (m, Ph, 39H), 2.33 (m, CH_2, 6H), 1.49 (q, $^4J_{HP}$ = 2.7, CH_3, 3H). 190 K: 7.7−6.9 (m, Ph, 45H), 2.30 (br, CH_2, 6H), 1.41 (br, CH_3, 3H). ^{13}C{^{1}H}, 298 K: 206.3 (d, CO trans to PPh_3, $^2J_{CP}$ = 28.3), 205.0 (dd, CO trans to P_3, $^2J_{CP}$ = 12.5), 203.5 (dd, cis, *cis*-CO, $^2J_{CP}$ = 7, 1.5), 137.0 (d, *i*-Ph(PPh_3), $^1J_{CP}$ = 37.2), 134.6 (d, *o*-Ph(PPh_3), $^2J_{CP}$ = 11.9), 130.0 (d, *p*-Ph(PPh_3), $^4J_{CP}$ = 1.5), 128.7 (s, *m*-Ph(PPh_3)), 138.2 (dd, *i*-Ph(triphos), $^2J_{CRh}$ = 18), 132.8 (br, *o*-Ph(triphos)), 129.7 (s, *p*-Ph(triphos)), 128.8 (s, *m*-Ph-(triphos)), 35.1 (m, CH_2), 39.2 (q, CH_3, $^3J_{PC}$ = 9.7), 38.4 (q, C, $^2J_{CP}$ = 6.5). IR [ν (cm^{-1}); CH_2Cl_2)]: 2012(s), 1906(vs), 1893(vs), 1858(s).

Crystal Structure Analyses. X-ray diffraction data for **5** and **6** were collected at room temperature on a Bruker rotating anode generator and platform-equipped with Goebel mirrors and CCD detector using Cu Kα radiation (λ = 1.541 84 Å). Crystal data and details about structure refinements are given in Table 6. Crystals of **5** were orange-red, and those of **6** were yellow. The dimensions of the crystals used for data collections were 0.05 mm × 0.20 mm × 0.80 mm (**5**) and 0.06 mm × 0.20 mm × 0.90 mm (**6**). Data were collected over the 6−115° 2θ range in both cases. Empirical absorption corrections were applied with SADABS [max/min transmission factors 1.000/0.409 (**5**) and 1.000/0.514 (**6**)].[26] The structures were solved by direct methods[27] and heavy-atom procedures;[28] drawings were made with ORTEP.[29] Compound **5** crystallizes with one toluene solvate molecule and **6** with two dichloromethane molecules per formula unit. The refinement was performed on F_o^2 for both structures. In the final model for **5** all non-hydrogen atoms, including those of the solvent and of the BF_4^- fractional sites (see below), were refined anisotropically. The toluene molecule was modeled by a benzene molecule with idealized geometry because no unique methyl position was detected. The BF_4^- anion was refined as two regular tetrahedral arrangements of F fractional atoms surrounding a unique B position; the two tetrahedra had complementary population parameters and independent B−F distances. A soft restraint was imposed on the phenyl C−C distances in the triphos ligand. Hydrogen atoms were in calculated positions, riding, with $U_H = 1.2U_C$ ($1.5U_C$ for methyl hydrogens), where U_C is the equivalent isotropic temperature factor of the carrier atom. The model for **6** was similar to that of the cation in **5** except that no restraint was imposed on the C−C distances of phenyl groups.

Table 6. Crystal Data, Data Collection, and Structure Refinement for the Compounds [{(triphos)Co}(μ,$\eta^{3:1}$-P_3){$Re(CO)_5$}]BF_4·C_7H_8 (**5**) and [{(triphos)Rh}(μ,$\eta^{3:1}$-P_3){$W(CO)_4PPh_3$}]·$2CH_2Cl_2$ (**6**)

	5	**6**
empirical formula	$C_{53}H_{47}BCoF_4O_5P_6Re$	$C_{65}H_{58}Cl_4O_4P_7RhW$
fw	1281.66	1548.47
cryst syst	monoclinic	monoclinic
space group	$P2_1/n$ (No. 14)	$P2_1/n$ (No. 14)
a (Å)	14.754(2)	14.872(3)
b (Å)	24.886(4)	27.317(6)
c (Å)	15.182(2)	16.992(4)
α (deg)	90	90
β (deg)	103.38(1)	111.75(5)
γ (deg)	90	90
V (Å^3)	5423(1)	6412(2)
T (°C)	20	20
Z	4	4
ρ_{calc} (g cm^{-3})	1.570	1.604
λ (Å)	1.54184 (Cu Kα)	1.54184 (Cu Kα)
μ (cm^{-1})	88.7	89.1
final R indices [$I > 2\sigma(I)$][a]	R1 = 0.053, wR2 = 0.123	R1 = 0.053, wR2 = 0.123
final R indices (for all data)[a]	R1 = 0.070, wR2 = 0.128	R1 = 0.074, wR2 = 0.130

[a] $R1 = (\sum||F_o| - |F_c||)/\sum|F_o|$, $R2 = \{\sum[w(F_o^2 - F_c^2)^2]/\sum[w(F_o^2)^2]\}^{1/2}$.

Acknowledgment. We acknowledge financial support by the Italian Ministero dell'Università e della Ricerca Scientifica e Tecnologica. The work has been enabled by support with a postdoctoral grant (M.P.E.) of the "Gemeinsamen Hochschul-sonderprogramm von Bund und Ländern" by the DAAD (German Academic Exchange Service). This work was supported by the European Commission (INCO ERB-IC 15C960746).

Supporting Information Available: X-ray crystallographic files, in CIF format, for compounds **5** and **6**. This material is available free of charge via the Internet at http://pubs.acs.org.

IC991380W

(24) Schmidt, S. P.; Nitschke, J.; Trogler, W. C. *Inorg. Synth.* **1989**, *26*, 113.
(25) Choi, M.-G.; Angelici, R. J. *J. Am. Chem. Soc.* **1990**, *112*, 7811.
(26) Sheldrick, G. M., Ed. *SADABS: Program for Empirical Absorption Corrections*; University of Göttingen: Göttingen, Germany, 1986.
(27) Altomare, A.; Burla, M. C.; Camalli, M.; Cascarano, G.; Giacovazzo, C.; Guagliardi, A.; Polidori, G. *J. Appl. Crystallogr.* **1994**, *27*, 435.
(28) Sheldrick, G. M. *SHELXL 93, Program for Crystal Structure Refinement*; University of Göttingen: Göttingen, Germany, 1993.
(29) Johnson, C. K. *ORTEP*; Report ORNL-5138; Oak Ridge National Laboratory: Oak Ridge, TN.